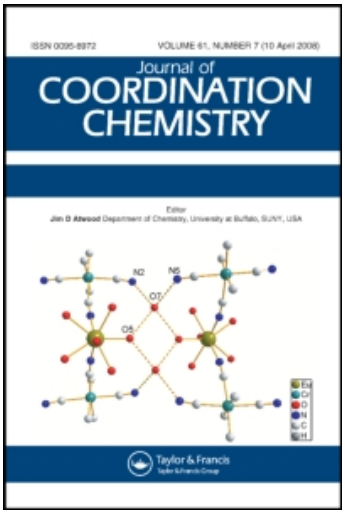

Journal of Coordination Chemistry
Publication details, including instructions for authors and subscription information:
http://www.informaworld.com/smpp/title~content=t713455674

Synthesis, characterization, X-ray structural analysis and study of oxidative properties of tetraethylammonium chlorochromate

Shahriare Ghammamy[a]; Wong Wing-Tak[b]; Kheiroallah Mehrani[c]; Monir Rahnama baghy[a]; Hamid Afrand[c]; Samaneh Dastpeyman[a]
[a] Faculty of Science, Department of Chemistry, Imam Khomeini International University, Ghazvin, Iran [b] Department of Chemistry, The University of Hong Kong, Pokfulam, Hong Kong SAR, P.R. CHINA [c] Faculty of Science, Department of Chemistry, Islamic Azad University, Ardebil, Iran

To cite this Article Ghammamy, Shahriare , Wing-Tak, Wong , Mehrani, Kheiroallah , Rahnama baghy, Monir , Afrand, Hamid and Dastpeyman, Samaneh(2008) 'Synthesis, characterization, X-ray structural analysis and study of oxidative properties of tetraethylammonium chlorochromate', Journal of Coordination Chemistry, 61: 20, 3225 — 3236
To link to this Article: DOI: 10.1080/00958970802020657
URL: http://dx.doi.org/10.1080/00958970802020657

Journal of Coordination Chemistry
Vol. 61, No. 20, 20 October 2008, 3225–3236

Taylor & Francis
Taylor & Francis Group

Synthesis, characterization, X-ray structural analysis and study of oxidative properties of tetraethylammonium chlorochromate

SHAHRIARE GHAMMAMY*†, WONG WING-TAK‡, KHEIROALLAH MEHRANI§, MONIR RAHNAMA BAGHY†, HAMID AFRAND§ and SAMANEH DASTPEYMAN†

†Faculty of Science, Department of Chemistry, Imam Khomeini International University, Ghazvin, Iran
‡Department of Chemistry, The University of Hong Kong, Pokfulam Road, Pokfulam, Hong Kong SAR, P.R. CHINA
§Faculty of Science, Department of Chemistry, Islamic Azad University, Ardebil Branch, Ardebil, Iran

(*Received 21 November 2006; in final form 18 August 2007*)

Tetraethylammonium chlorochromate(VI), $Et_4N[CrO_3Cl]$ is easily synthesized in nearly quantitative yield using a direct reaction of chromium(VI) oxide and tetraethylammonium chloride and characterized by elemental analysis, IR, UV/Visible, ^{1}H-NMR and ^{13}C-NMR techniques and single-crystal X-ray diffraction analysis (monoclinic system, space group C2(#5), with $a = 12.023(3)$, $b = 7.998(2)$, $c = 14.527(4)$ Å, $\beta = 114.187(4)^\circ$, $V = 1274.4(6)$ Å^3 and $Z = 4$). X-ray data determined the CH···O hydrogen bond that forms between the ethyl hydrogen of the cation and oxygen of the anion. This compound is a versatile reagent for efficient and selective oxidation of organic substrates, in particular for alcohols to their corresponding aldehydes or ketones, under mild conditions.

Keywords: Tetraethylammonium chlorochromate; Synthesis; Characterization; X-ray structural analysis; Oxidative properties

1. Introduction

Chromium(VI) is the most widely employed among oxidizing agents based on high-valent transition metal oxo derivatives such as reagents derived from ruthenium, osmium, iron, manganese, vanadium and molybdenum. Chromium(VI) is a versatile oxidant for many types of substrates from metal ions to naturally occurring organic compounds, and has a wide range of applications spanning synthesis of sulfur nanoparticles and determination of biological oxygen demand in organic polluted

*Corresponding author. Email: shghamamy@yahoo.com

ISSN 0095-8972 print/ISSN 1029-0389 online © 2008 Taylor & Francis
DOI: 10.1080/00958970802020657

water [1]. There is continued interest in the development of new chromium(VI) reagents for effective and selective oxidation of organic substrates, in particular alcohols, under mild conditions. Significant improvements were achieved by use of new oxidizing agents such as N-methylbenzylammonium fluorochromate [2], pyridinium fluorochromate [3], triphenylmethylphosphonium chlorochromate [4], benzyltrimethylammonium fluorochromate [5] and quinolinium fluorochromate [6]. There were some primary incentives for selection of Et_4N^+ as the counter ion in the work reported in this manuscript. First, quaternary ions such as ammonium are often used as phase transfer catalysts, perhaps making tetraethylammonium chlorochromate(VI), $Et_4N[CrO_3Cl]$, TEACC, a more efficient and stronger oxidizing agent. This new compound (figure 1) is more efficient for quantitative oxidation of several organic substrates and has certain advantages over similar oxidizing agents in terms of the amount of oxidant and solvent required, short reaction times and high yields. Second, quaternary ions such as ammonium are used as crystal growing agents. Hence, using this counter ion improves the quality of the TEACC crystals. This compound crystallized and was structurally characterized by X-ray diffraction. Furthermore, this compound does not react with MeCN, a suitable medium for studying kinetics and mechanism.

2. Experimental

2.1. *Material and instruments*

CrO_3 (Merck, p.a.) was used without purification. Solvents were purified by standard methods. Infrared spectra were recorded as KBr disks on a Shimadzu model 420 spectrophotometer. UV/Visible measurements were made on an Uvicon model 922 spectrometer. ^{1}H-NMR and ^{13}C-NMR were recorded on a Bruker AVANCE DRX 500 spectrometer at 500 and 125 MHz, respectively, in CD_3CN solutions. All chemical shifts are quoted in ppm using the high-frequency positive convention; ^{1}H-NMR and ^{13}C-NMR spectra were referenced to external $SiMe_4$. Chromium was estimated iodometrically. After oxidation of organic substrates, chromium was determined by reoxidizing with acidic potassium peroxodisulfate ($K_2S_2O_8$) solution. The percent composition of elements was obtained from the Microanalytical Laboratories, Department of Chemistry, OIRC, Tehran.

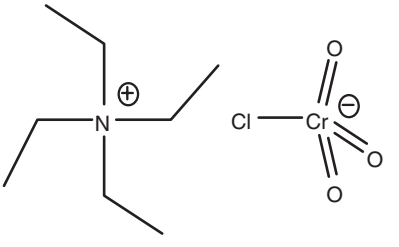

Figure 1. A view of the formula unit of TEACC.

Table 1. Crystal data and structure refinement summary for TEACC.

CCDC deposit no.	625098
Empirical formula	$C_8H_{20}ClCrNO_3$
Formula weight	265.7
Crystal dimensions (mms)	$0.14 \times 0.18 \times 0.42$
Crystal system, space group	Monoclinic, C2 (#5)
a (Å)	12.023(3)
b (Å)	7.998(2)
c (Å)	14.527(4)
b (°)	114.187(4)
V (Å^3)	1274.4(6)
Z	4
D_{Calcd} (g cm^{-3})	1.385
$F(000)$	560
m(Mo-Kα)(cm^{-1})	10.92
T(°C)	$28 + 1$
Wavelength (Å)	0.71073
Reflections collected/unique	3974/1541 ($R_{int} = 0.019$)
Number of observations ($I > 2.00s(I)$)	1213
Number of variables	149
Reflection/parameter ratio	8.14
Residuals: R ($I > 2.00s(I)$)	0.048
Residuals: R_w ($I > 2.00s(I)$)	0.052
Goodness of fit indicator	1.014
Flack parameter (Friedel Pairs = 0)	−0.1(1)
Max shift/error in final cycle	0.043
Maximum peak in final diff. map (e$^-$ Å^{-3})	0.87
Minimum peak in final diff. Map (e$^-$ Å^{-3})	−0.23

2.2. *Synthesis of tetraethylammonium chlorochromate(VI), $Et_4N[CrO_3Cl]$*

To a solution of tetraethylammonium chloride (1.65 g, 1 mmol) in MeCN (15 mL) was added a solution of CrO_3 (1 g, 1 mmol) in MeCN (10 mL) under stirring at room temperature until an orange precipitate formed. After 1 h stirring, the mixture was filtered, washed with hexane (2×15 mL), and dried at room temperature. Table 1 shows the assignment of UV/visible spectrum, consistent with the TEACC structure. Also IR, ^{1}H-NMR and ^{13}C-NMR (in CD_3CN solutions) were consistent with the TEACC structure. mp, 120 °C. Anal. Calcd for $C_8H_{20}ClCrNO_3$ (%): C, 36.16; H, 7.53; N, 5.27. Found: C, 36.83; H, 7.81; N, 5.53. ^{1}H-NMR (500 MHZ, CD_3CN): $\delta = 1.27$ (t, 3H, –CH_3), $\delta = 3.25$ ppm (q, 2H, –CH_2–), ^{13}C–NMR (125 MHZ, CD_3CN): δ 8.10, 53.35.

2.3. *Crystallographic measurements and structure determination*

The data were collected at a temperature of 28 ± 1 °C to a maximum 2Θ value of 54.9°. A total of 1270 oscillation images were collected. A sweep of data was done using ω scans from 332.0 to 150.2° in −0.3° steps, at $\chi = 54.7°$ and $\varphi = 0.0°$. The exposure rate was 50.0 [sec./°]. The detector swing angle was −28.00°. A second sweep was performed using ω scans from 332.0 to 210.5° in −0.3° steps, at $\chi = 54.7°$ and $\varphi = 90.0°$. The exposure rate was 50.0 [sec./°]. The detector swing angle was −28.00°. Another sweep was performed using ω scans from 332.0 to 263.0° in −0.3° steps, at $\chi = 54.7°$ and $\varphi = 180.0°$. The exposure rate was 50.0 [sec./°]. The detector swing angle was −28.00°. Another sweep was performed using ω scans from 332.0 to 317.0° in −0.3° steps, at

Table 2. Selected bond lengths (Å).

Cr(1)–Cl(2)	2.184(2)	Cr(1)–O(1)	1.601(5)
Cr(1)–O(2)	1.626(8)	Cr(1)–O(3)	1.598(9)
N(1)–C(1)	1.516(9)	N(1)–C(1)#1	1.516(9)
N(1)–C(3)	1.519(9)	N(1) C(3)#1	1.519(9)
N(2)–C(5)	1.522(9)	N(2) C(5)#2	1.522(9)
N(2)–C(7)	1.534(9)	N(2)–C(7)#2	1.534(9)
C(1)–C(2)	1.53(1)	C(1)–H(1)	0.95
C(1)–H(2)	0.95	C(2) H(3)	0.95
C(3)–C(4)	1.51(1)	C(5)–C(6)	1.54(1)
C(6)–H(14)	0.9499	C(7)–C(8)	1.50(1)

Symmetry operators: #1. $-X$, Y; $-Z$. #2. $-X+1$, Y, $-Z+1$.

Table 3. Selected bond angles (°).

O(1)–Cr(1)–Cl(2)	108.5(2)	O(2)–Cr(1)–Cl(2)	108.2(3)
O(3)–Cr(1)–Cl(2)	107.6(3)	O(2)–Cr(1)–O(1)	110.9(4)
O(3)–Cr(1)–O(1)	110.5(4)	O(3)–Cr(1)–O(2)	111.0(4)
C(1)#1–N(1)–C(1)	106.8(7)	N(1)–C(1)–C(2)	115.2(6)
C(3)–N(1)–C(1)	110.7(4)	C(3)#1–N(1)–C(1)	110.3(5)
N(1)–C(1)#1–C(2)#1	115.2(6)	C(3)–N(1)–C(1)#1	110.3(5)
C(3)#1–N(1)–C(1)#1	110.7(4)	N(1)–C(1)#1–H(1)#1	108
N(1)–C(1)#1–H(2)#1	108	C(3)#1–N(1)–C(3)	108.0(7)
N(1)–C(3)–H(7)	107.8	N(1)–C(3)#1–C(4)#1	115.9(7)
N(1)–C(3)#1–H(6)#1	107.8	N(1)–C(3)1)–H(7)#1	107.8
N(2)–C(5)–H(11)	108.4	C(5)#2–N(2)–C(5)	111.3(7)
C(7)#2–N(2)–C(5)	106.8(3)	N(2)–C(5)–H(12)	108.4
N(2)–C(5)#2–C(6)#2	113.9(5)	C(7)–N(2)–C(5)#2	106.8(3)
C(7)#2–N(2)–C(5)#2	110.5(4)	N(2)–C(5)#2–H(11)#2	108.4
N(2)–C(5)#2–H(12)#2	108.4	N(2)–C(7)#2–H(16)#2	108.1
N(2)–C(7)–H(16)	108.1	C(7)2)–N(2)–C(7)	111.0(7)
N(2)–C(7)#2–C(8)#2	115.0(5)	N(2)–C(7)–H(17)#2	108.1

Symmetry operators: #1. $-X$, Y, $-Z$ #2. $-X+1$, Y, $-Z+1$.

$\chi = 54.7°$ and $\varphi = 0.0°$. The exposure rate was 50.0 [sec./°]. The detector swing angle was $-28.0°$. The crystal-to-detector distance was 50.00 mm.

Of the 3974 reflections collected, 1541 were unique ($R_{int} = 0.019$); equivalent reflections were merged. Data were collected and processed by using CrystalClear, Rigaku [7]. Net intensities and sigmas were derived as follows: $F^2 = [\Sigma(P_i - mB_{ave})] \times {L_p}^{-1}$, where P_i is the value in counts of the ith pixel, m is the number of pixels in the integration area, B_{ave} is the background average, Lp is the Lorentz and polarization factor. $B_{ave} = \Sigma(B_j)/n$, where n is the number of pixels in the background area, B_j is the value of the jth pixel in counts. $\sigma^2(F^2{}_{hkl}) = [(\Sigma P_i) + m((\Sigma(B_{ave} - B_j)^2)/(n-1))] \times L_p \times \text{errmul} + (\text{erradd} \times F^2)^2$, where erradd = 0.00, errmul = 1.00. The linear absorption coefficient, μ, for Mo-Kα radiation is 10.9 cm^{-1}, resulting in transmission factors ranging from 0.71 to 1.00. The data were corrected for Lorentz and polarization effects.

The structure was solved by direct methods [8] and expanded using Fourier techniques [9]. The non-hydrogen atoms were refined anisotropically. Hydrogens were placed at geometrical positions with C–H = 0.95 Å and refined using the riding model, $U_{iso}(H) = U_{eq}(C)$. The final cycle of full-matrix least-squares refinement (least

Table 4. Oxidation data of alcohols with TEACC.

Substrate	Product	Time (min)	Yield (%)
n–C_3H_7–OH	*n*–C_2H_5–CHO	120	92
2–C_3H_7–OH	2–C_2H_6–CO	85	95
n–C_4H_9–OH	*n*–C_3H_7–CHO	118	89
2-C_4H_9–OH	2–C_3H_8–CHO	85	94
n–C_5H_{11}–OH	*n*–C_4H_9–CHO	88	97
n-Octanol	*n*-Octanal	100	96
Cyclohexanol	Cyclohexanone	95	98
$PhCH_2OH$	PhCHO	40	98

squares function minimized: $\Sigma w(|F_o| - |F_c|)^2$, where w = least squares weights) on F was converged (largest parameter shift was 0.04 times its esd) with unweighted and weighted agreement factors of: $R = \Sigma||F_o| - |F_c||\Sigma|F_o| = 0.048$, $R_w = [\Sigma w(|F_o| - |F_c|)^2/\Sigma w F_0^2]^{1/2} = 0.052$. The standard deviation of an observation of unit weight (standard deviation of an observation of unit weight: $[\Sigma w\ (|F_o| - |F_c|)^2/(N_o - N_v)]^{1/2}$, where N_o = number of observations, N_v = number of variables) was 1.01. A Sheldrick weighting scheme was used. Plots of $\Sigma w(|F_o| - |F_c|)^2$ *versus* $|F_o|$, reflection order in data collection, sin Θ/λ and various classes of indices showed no unusual trends. The Flack parameter 6 is $-0.1(1)$ and the Friedel pairs is 0. Neutral atom scattering factors were taken from Cromer and Waber [10]. Anomalous dispersion effects were included in F_{calc} [11]; the values for $\Delta f'$ and $\Delta f''$ were those of Creagh and McAuley [12]. The values for the mass attenuation coefficients are those of Creagh and Hubbell [13]. All calculations were performed using the CrystalStructure and crystallographic software package, Rigaku [14, 15]. Crystallographic data and experimental details for structural analysis are summarized in table 1 and selected bond lengths, angles and torsion angles are presented in tables 2 and 3, respectively.

2.4. *General procedure for oxidation of some organic substrates with tetraethylammonium chlorochromate(VI)*

In a small-scale experiment, TEACC (2.65 g, 1 mmol) was poured in MeCN (2–10 mL, 0.8 gcm^{-3}) and an alcohol (1 mmol in 0.5 to 1.5 mL of MeCN) such as benzyl alcohol was added dropwise at room temperature. The mole ratio of substrate to oxidant was 1 : 1 (see table 4). [The progress and completion of the reaction was monitored and checked by UV/Visible and TLC using ether/petroleum ether (60/40) as eluant.] The amount of the oxidant during the reaction was measured spectrophotometrically at 363 nm. A very small magnetic stirrer was designed for the cell (10 mm quartz cell) compartment to stir the solution under study in the cell. The reaction mixtures remained homogenous. The mixture was diluted with ether (1 : 1 vol/vol) and filtered through a short column of silica gel to give a clear solution. The solution was evaporated and the residual product purified by distillation, recrystallization or column chromatography. Analysis of the mixture for corresponding carbonyl compounds was accomplished by the procedure reported in earlier papers [3–6] (Supplementary Data).

3. Results and discussion

3.1. *Oxidation and general characterization*

$Et_4N[CrO_3Cl]$ was prepared by the reaction of Et_4NCl and CrO_3 in a 1:1 ratio in MeCN as follows:

$$Et_4NCl + CrO_3 \rightarrow Et_4N[CrO_3Cl]$$

Oxidations obtained with tetraethylammonium chlorochromate(VI) are very satisfactory and show the new reagent to be a valuable addition to existing oxidizing agents.

The inequality between the Cr–O and Cr–Cl bonds clearly demonstrated by our X-ray data is responsible for higher reactivity of TEACC. The reason for this inequality is due to the CH···O hydrogen bond that forms between the ethyl hydrogen of the cation and oxygen of the anion. TEACC appears to be a stronger reagent possibly due to its lower symmetry and has advantages over similar oxidizing agents in terms of amounts of oxidant and solvent required, in short reaction times required and in higher product yields. TEACC in MeCN oxidizes primary and secondary alcohols to, respectively, the corresponding aldehydes or ketones in high yields (table 4).

The IR spectrum is similar to those of other chlorochromates [16, 17]. TEACC is soluble in water, dichloromethane, acetonitrile, methanol, ethanol, propanol, acetone and acetic acid; it is not soluble in benzene, diethyl ether, toluene and cyclohexane.

3.2. *X-ray structure*

The compound was crystallized by slow evaporation from MeCN after one week. A red block crystal was mounted on a glass fiber and all measurements were made on a Bruker SMART CCD area detector with graphite monochromated Mo-Kα radiation ($\lambda = 0.71073$ Å). Cell constants and an orientation matrix for data collection corresponded to a C-centered monoclinic cell. Based on the systematic absences of: *hkl*: $h + k \pm 2n$. The tetraethylammonium cations are located in two different symmetry environments. The cation and anion moieties are separated from each other and arranged in a C-centered lattice with the tetraethylammonium cation located at the midpoint of the edges of the unit cell. The shortest Cr···Cr distance is 7.220(3) Å. The Cr(VI) is tetragonally coordinated by three oxygen atoms Cr–O = 1.598(9)–1.625(8) Å and one chloride, Cr–Cl = 2.184(2) Å. Geometry about the Cr(1) is a distorted tetrahedron with six unique bond angles around this atom. X-ray data clearly demonstrate such inequality (figures 2 and 3).

From simple VSEPR theory, the repulsion between double bonds is stronger than that between a single and a double bond. The three unique O–Cr(1)=O bond angles of 110.5(4), 110.9(4) and 111.0(4) are greater than the corresponding Cl–Cr(1)–O bond angles with 107.6(3), 108.2(3) and 108.5(2) amounts. The Cr(1)–O(2) length [1.626(8) Å] is 0.025 Å longer than that of the Cr(1)–O(1) length [1.601(5) Å], or 0.028 Å longer than that of the Cr(1)–O(3) length [1.598(9) Å]. All of these values show double bond character, but Cr(1)–O(2) is longer than the others with less double bond character. The X-ray model suggests structural distortions away from idealized C_{3V} geometry due to the CH···O hydrogen bond that forms between the ethyl hydrogen and O(2). The data

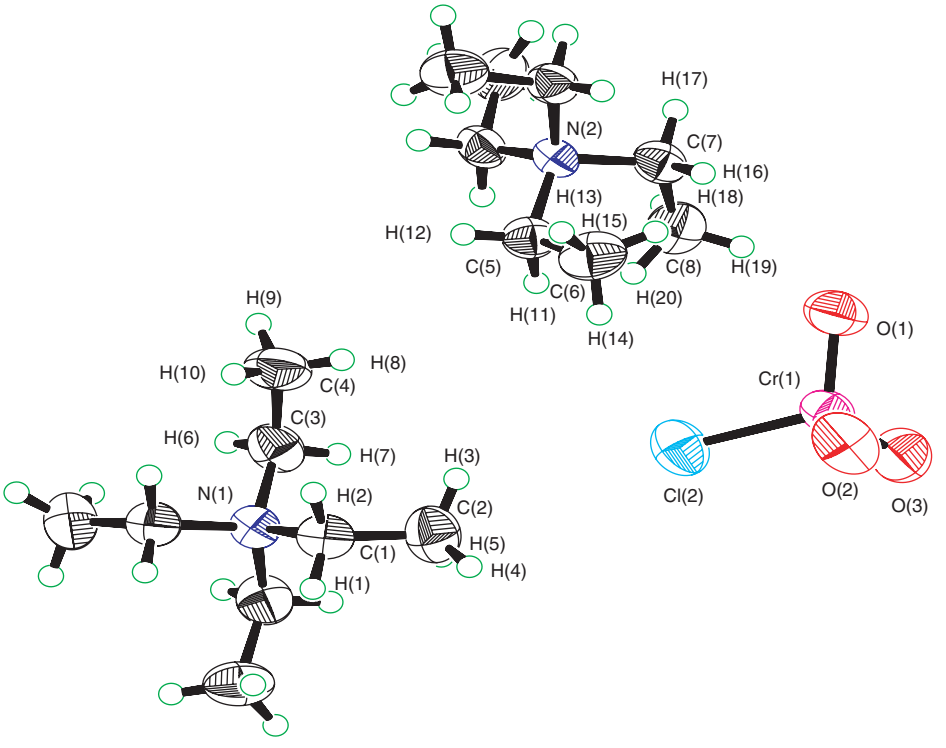

Figure 2. ORTEP diagram of $Et_4N[CrO_3Cl]$.

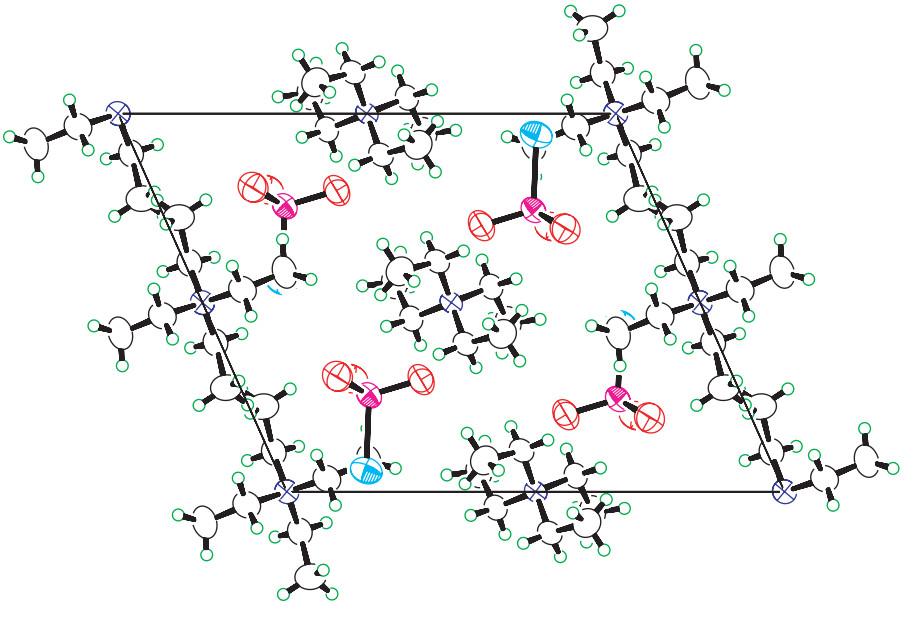

Figure 3. The unit cell of $Et_4N[CrO_3Cl]$.

for hydrogen bonds are collected in table 5. This structure is similar to McGrady systems in that the presence of π donor ligands make larger angles [18].

3.3. *IR and UV spectra*

The electronic spectrum of TEACC in acetonitrile is shown in figure 4. The transitions in CrO_3Cl^- are charge transfer [17], with three electronic transitions summarized in table 6.

(a) Based on CrO_4^{2-} and the correlation $t_1(T_d) \rightarrow a_2 + e(C_{3v})$, the highest filled orbitals in CrO_3Cl^- are anticipated to have a_2 and e symmetry. The a_2 orbital has the higher energy, a node at the halogen and only slight chromium character. Hence, the highest occupied orbital retains an oxygen lone-pair description. The highest filled e orbital has somewhat greater, although still small, chromium character and a significant halogen contribution. The latter is expected from e.g., the relative electronegativities, which should tend to concentrate the chlorine character in lower energy levels. The lowest unoccupied level has e symmetry and predominantly chromium 3d character, as anticipated from the correlation $e(T_d) \rightarrow e(C_{3v})$.

Table 5. Hydrogen bond interactions (°).

D–H···A	d(D–H)	d(H···A)	d(D···A)	∠(DHA)
C(1)–H(2)···O(3)	0.95	2.59	3.349(11)	138

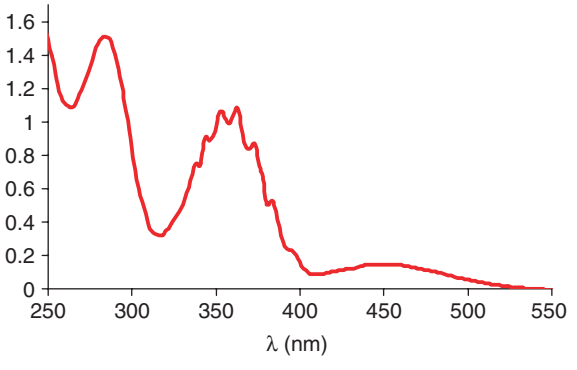

Figure 4. The electronic spectrum of TEACC in acetonitrile.

Table 6. UV-visible transitions.

$\lambda_{C.T}$(LMCT) (ε, $M^{-1}cm^{-1}$)	$\lambda_{C.T}$(LMCT) (ε, $M^{-1}cm^{-1}$)	$\lambda_{C.T}$(LMCT) (ε, $M^{-1}cm^{-1}$)
456	345	276
(135)	(690)	(1240)
$1a_2 \rightarrow 9e$	$8e \rightarrow 9e$	$12a_1 \rightarrow 9e$

Its chromium contribution decreases and its oxygen contribution increases in the order of CrO_4^{2-}, CrO_3F^-, CrO_3Cl^-, but the changes are small; the halogen contribution is very small and similar in both halochromates.

(b) The spectral correlation between CrO_4^{2-} and CrO_3Cl^- is very good. The low lying $^1T_1$ state of CrO_4^{2-} should split into a ^1E state and a $^1A_2$, and, as the $^1A_1 \rightarrow {}^1A_2$ transition is forbidden in C_{3v} symmetry, we should observe $^1A_1 \rightarrow {}^1E$ more prominently. A $^1T_2$ state, on the other hand, should split into ^1E and $^1A_1$ states. The spectral results allow us to conclude that replacement of an oxide ligand by a chloride has almost no effect on a tetrahedral t_1 orbital; to a good approximation it remains oxygen-localized and non-bonding. For the second $^1A_1 \rightarrow {}^1T_2$ transition of CrO_4^{2-}, however, the situation is quite different. The MO scheme for MO_4^{n-}complexes shows that there are three filled π-orbitals generated from oxide 2p-orbitals, e, t_2 and t_1. An e orbital is strongly π-bonding, t_1 is non-bonding, and t_2 is nearly non-bonding. Upon replacement of an oxide by a halide, strong t_2 splitting to orbitals of e and a_1 symmetries is expected, as the e orbital will have halide pπ character [17–19].

The assignments of the IR spectrum in table 7 refer to the cation and anion with distorted T_d and C_{3v} symmetries, respectively. The IR spectrum of this compound should have some additional bands because of the distortion from tetrahedral and C_{3v} symmetries for the cation and the anion, respectively. The XY_3Z ions have six infrared active vibrations. These infrared active vibrations are $\nu_1(A_1)$ or $\nu(XY_3)$, $\nu_2(A_1)$ or $\nu(XZ)$, $\nu_3(A_1)$ or $\delta(XY_3)$, $\nu_4(E)$ or $\nu(XY_3)$, $\nu_5(E)$ or $\delta(XY_3)$ and $\nu_6(E)$ or $\rho_r(XY_3)$. In TEACC, $\nu_1(A_1)$ or $\nu(XY_3)$, $\nu_2(A_1)$ or $\nu(XZ)$ and $\nu_4(E)$ or $\nu(XY_3)$ are seen at 894, 445 and 945 cm^{-1}, respectively.

The following are the main points from the vibronic transitions (table 8 and Supplementary Data):

(a) Vibrational assignments were made after examination of the region just above 300 nm and table 8 shows the vibronic intervals. As seen these data are not equal with any of the CrO_3Cl^- ground state vibrational frequencies. Vibrational intervals in the electronic spectra have been assigned by the reference to the ground state values on the assumption that they correspond to the totally symmetric modes. It is assumed that these intervals are related to excited symmetric stretching mode in the CrO_3 group. The CrO_3 ground state symmetric stretching frequency is 890–911 cm^{-1} in CrO_3Cl^- and significantly lower in the excited state. Therefore,

Table 7. The frequencies (cm^{-1}) and assignment of cation and anion of TEACC.

ν (cm^{-1})	Assignment $[Et_4N]^+$	Intensity	ν (cm^{-1})	Assignment	Intensity
3430	$\nu_{CH3} + \nu_{19}$	(w, br.)	1470	ν_{16}	(s)
3370	$\nu_{CH3} + \nu_8$	(w, br.)	1400	ν_{16}	(m)
3102	ν_{CH3}, asym. str	(m)	1279	ν_{rock}	(w)
3015	ν_{13}, ν_{CH3}, asym. str	(s)	940	ν_{18}	(Vs.)
2990	ν_{14}, ν_{CH3}, asym. str	(w, br.)	470	ν_{19}	(m)
2772	ν_{14}, ν_{CH3}, asym. str	(s, br.)	446	ν_{19}	(m)
2640	$\nu_7 + \nu_{16}$	(w.)		$[CrO_3Cl]^-$	
2470	$\nu_3 + \nu_8 + \nu_{16}$	(w.)	945	ν_{as} Cr=O (E)	(s)
1838	$\nu_8 + \nu_{15}$	(w, br.)	894	ν_s Cr=O (A1)	(s)
			445	ν Cr–Cl (A1)	(s)

Table 8. The measured center frequencies and the vibrational spacings (in cm^{-1}) for CrO_3Cl^- of TEACC in acetonitrile.

Number	λ	Assignment	$\nu_{cm}{}^{-1}$	$\Delta\nu_{cm}{}^{-1}$	
1	396	$0 \rightarrow 0$	25252.52		$\nu_{max} \pm 10 =$ 27472.52
2	384	$0 \rightarrow 1$	25974.02	721.5	
3	374	$0 \rightarrow 2$	26737.96	763.94	$20 \pm \nu_{vib} =$ 751.56
4	363	$0 \rightarrow 3$	27548.2	810.24	
5	354	$0 \rightarrow 4$	28248.58	700.38	
6	345	$0 \rightarrow 5$	28985.5	736.92	$\nu_{00} \pm 50 =$ 25252.52
7	336	$0 \rightarrow 6$	29761.9	776.4	

excited state bonds are weaker and probably longer than ground state. Reductions of frequencies of 10–20 percent observed in the excited states are of about the same magnitude as found in the spectra of MO_4^- complexes.

(b) The vibronic intervals in this compound showed that higher-order coupling has been induced. The second (W) and third (Y) order coupling terms in the displacement are also included. Their inclusion has a marked effect on the vibrational energies. The anharmonicity is now considerable and the calculated results show a clear resemblance to these experimentally observed for CrO_3Cl^- [19].

(c) The decreasing Cr=O stretching frequency in the excited state confirms anharmonicity. The increasing of bond distance in excited state is shown the breakdown of adiabatic approximations. A very similar approach may be used to determine the molecular wave function corrected for the breakdown of the Born-Oppenheimer (BO) adiabatic approximation.

(d) This compound does not show any vibronic-spin-orbit coupling because of lowered symmetry. Decreasing symmetry from T_d of $CrO_4^{2-}$to C_{3v} of CrO_3Cl^- gives no triplet state or vibronic and spin-orbit coupling or vibronic-spin-orbit coupling [19].

(e) ν_{max} in CrO_3Cl^- occurs near ν_{03}, while in CrO_3F^- the peak is near ν_{05}. ν_{max} would occur at ν_{00} if bonds were the same lengths in both ground and excited electronic states. In order for ν_{max} to occur at higher vibrational levels in CrO_3F^-, it is necessary for the F^- substituent either to weaken the upper state Cr–O bonds or to strengthen the lower state Cr–O bonds relative to Cl^- and other ligands.

4. Conclusion

$Et_4N[CrO_3Cl]$ was synthesized, crystallized and characterized by elemental analysis, IR, UV/Visible, ^{1}H-NMR and ^{13}C-NMR techniques and single-crystal X-ray diffraction analysis. Additional bands have appeared in IR spectrum because of the distortion from tetrahedral and C_{3v} symmetries for the cation and the anion, respectively. The distortion is due to the CH $\cdots$ O hydrogen bond that forms between the ethyl hydrogen and oxygen atom. The X-ray experiment confirms distortions away from idealized C_{3V} geometry. This hydrogen bonding leads to different Cr–O and Cr–Cl lengths that help

to solve the crystal structure accurately and give a strong oxidation reagent. TEACC has certain advantages in terms of amounts of oxidant and solvent, short reaction times, no further oxidation to the corresponding carboxylic acids, no Lewis acid catalyst, reaction under non-aqueous conditions and in higher product yields. Because of the stability and solubility of TEACC, the reactions can be performed at room temperature and the separation of the products is facile. During the reactions, the color of the oxidant changes from orange to brown, providing visual means for ascertaining the progress of the oxidation. The reactions under non-aqueous condition make this reagent a useful method for oxidation of alcohols.

Supplementary material

Crystallographic data have been deposited with the Cambridge Crystallographic Data Center with the deposited numbers CCDC Number 625098. Copies of this information may be obtained free of charge from The Director, CCDC, 12 Union Road, Cambridge, CB2 1EZ, UK (Fax: +44-1223-336033; Email: deposit@ccdc.cam.ac.uk).

Acknowledgements

The authors would like to thank Dr. Gh. Rezaei Behbahani and Dr Mahjoub for valuable discussions.

References

[1] H.C. Brown, C. GunduRao, S.U. Kulkarni. *J. Org. Chem.*, **44**, 2809 (1979).
[2] M.Z. Kassaee, S.Z. Sayyed-Alangi, H. Sajjadi-Ghotbabadi. *Molecules*, **9**, 825 (2004).
[3] K.K. Banerji, V. Sharma, P.K. Sharma. *J. Chem. Research (S)*, 290 (1996).
[4] A.R. Hajipour, L. Khazdooz, A.E. Ruoho. *J. Iranian Chem. Soc.*, **2**, 315 (2005).
[5] M.Z. Kassaee, M. Hattami, L. Moradi. *Acta Chim. Slov.*, **51**, 743 (2004).
[6] U. Bora, M.K. Chaudhuri. *Tetrahedron*, **57**, 2445 (2001).
[7] Rigaku/MSC, *Single Crystal Structure Analysis Software*, Version 3.00. Rigaku/MSC, 9009 New Trails Drive, The Woodlands, TX, USA, 77381-5209. Rigaku, 3-9-12 Akishima, Tokyo 196-8666, Japan.
[8] G.M. Sheldrick. *SADABS and SHELXS-97*, Gottingen University, Gottingen, Germany (1997).
[9] DIRDIF-99: P.T. Beurskens, G. Admiraal, G. Beurskens, W.P. Bosman, R. de Gelder, R. Israel, J.M.M. Smits. *The DIRDIF-99 program system, Technical Report of the Crystallography Laboratory*, University of Nijmegen, The Netherlands (1999).
[10] D.T. Cromer, J.T. Waber. *International Tables for X-ray Crystallography*, Table 2.2 A, Vol. 4, The Kynoch Press, Birmingham, England, (1974).
[11] J.A. Ibers, W.C. Hamilton. *Acta Crystallogr.*, **17**, 781 (1964).
[12] D.C. Creagh, W.J. McAuley. *International Tables for Crystallography,* Table 4.2.6.8, A.J.C. Wilson (Ed.), p. 219, Kluwer Academic Publishers, Boston (1992).
[13] D.C. Creagh, J.H. Hubbell. *International Tables for Crystallography,* Table 4.2.4.3, A.J.C. Wilson (Ed.), p. 200, Kluwer Academic Publishers, Boston (1992).
[14] Rigaku/MSC and Rigaku Corporation. Crystal Structure, *Single Crystal Structure Analysis Software*, V. 3.6.0 (2004).
[15] D.J. Watkin, C.K. Prout, J.R. Carruthers, P.W. Betteridge. *CRYSTALS Issue 10, Chemical Crystallography Laborator*, Oxford, UK (1996).

[16] K. Nakamoto. *Infrared and Raman Spectra of Inorganic and Coordination Compounds*, 3rd Edn, Vol. 1, pp. 70–124, Wiley, New York (1978), 140.
[17] S. Ghammamy, M. Rahnamabaghy. *Transition Met. Chem.*, **32**, 456 (2007).
[18] A. Haaland, W. Scherer, H.V. Volden, H.P. Verne, O. Gropen, G.S. McGrady, A.J. Downs, G. Dierker, W.A. Herrmann, P.W. Roesky, M.R. Geisberger. *Organometallics*, **19**, 22 (2000).
[19] G. Fischer. *Vibronic Coupling – The Interaction between the Electronic and Nuclear Motions*, pp. 120–153, Academic Press, Oxford, UK (1984).